



OPEN

A novel molecule Me6TREN promotes angiogenesis via enhancing endothelial progenitor cell mobilization and recruitment

SUBJECT AREAS:

STEM-CELL RESEARCH

SMALL MOLECULES

ANGIOGENESIS

EXPERIMENTAL MODELS OF
DISEASEReceived
20 June 2014Accepted
11 August 2014Published
28 August 2014

Correspondence and requests for materials should be addressed to Y.L. (shirlylyh@126.com) or X.P. (peixt@nic.bmi.ac.cn)

Haixu Chen^{1,2}, Sihan Wang^{1,2}, Jing Zhang^{1,2}, Xiangliang Ren^{1,2}, Rui Zhang^{1,2}, Wei Shi^{1,2}, Yang Lv^{1,2}, Yong Zhou³, Xinlong Yan^{1,2}, Lin Chen^{1,2}, Lijuan He^{1,2}, Bowen Zhang^{1,2}, Xue Nan^{1,2}, Wen Yue^{1,2}, Yanhua Li^{1,2} & Xuetao Pei^{1,2}

¹Stem Cell and Regenerative Medicine Lab, Beijing Institute of Transfusion Medicine, Beijing 100850, China, ²South China Research Center for Stem Cell & Regenerative Medicine, AMMS, Guangzhou 510005, China, ³Laboratory of Blood-borne Virus, Beijing Institute of Transfusion Medicine, Beijing 100850, China.

Critical limb ischaemia is the most severe clinical manifestation of peripheral arterial disease. The circulating endothelial progenitor cells (EPCs) play important roles in angiogenesis and ischemic tissue repair. The increase of circulating EPC numbers by using mobilization agents is critical for obtaining a better therapeutic outcome in patients with ischemic disease. Here, we firstly report a novel small molecule, Me6TREN (Me6), can efficiently mobilize EPCs into the blood circulation. Single injection of Me6 induced a long-lasting increase in circulating Flk-1⁺ Sca-1⁺ EPC numbers. In a mouse hind limb ischemia (HLI) model, local intramuscular transplantation of these Me6-mobilized cells accelerated the blood flow restoration in the ischemic muscles. More importantly, systemic administration of Me6 notably increased the capillary density, arteriole density and regenerative muscle weight in the ischemic tissue of HLI. Mechanistically, we found Me6 reduced stromal cell-derived factor-1 α level in bone marrow by up-regulation of matrix metalloproteinase-9 expression, which allowed the dissemination of EPCs into peripheral blood. These data indicate that Me6 may represent a potentially useful therapy for ischemic disease via enhancing autologous EPC recruitment and promote angiogenesis.

Large numbers of patients worldwide are suffering from ischemic damage diseases, including myocardial ischemia, stroke and critical limb ischemia (CLI). Novel therapeutic approaches have been developed for achieving ideal outcome of these ischemic diseases¹. Promoting angiogenesis by injection of angiogenic factors, or through direct implantation of endothelial progenitor cells (EPCs), is a viable therapeutic option to repair ischemic tissue. EPCs can augment neovascularization in ischemia diseases for which ischemic tissues require reperfusion around occluded vessels to recover their function. Several studies have shown that EPCs from peripheral blood (PB) or bone marrow (BM) promote angiogenesis and increase blood flow recovery in damaged tissues of HLI animal models²⁻⁴. Recent reports have suggested that EPCs in PB could serve as an endothelial reserve with the capacity to repair damaged vascular endothelium⁵⁻⁷. However, under steady-state conditions, EPCs circulate in the PB at very low frequencies that are insufficient for ischemic tissue repair^{8,9}. An efficient therapeutic strategy is to mobilize more EPCs into PB with pharmacological agents, which would lead to the incorporation of more EPCs into the ischemic tissue to enhance angiogenesis.

EPCs are known to be mobilized from the BM in response to various stimuli, including cytokines, chemokines, CXC chemokine receptor 4 (CXCR4) antagonists AMD3100, and nitric oxide¹⁰⁻¹⁷. Among these agents, AMD3100 is the only small molecule drug proved to have the function in mobilizing EPCs and enhancing angiogenesis in ischemic mice. The therapeutic effect of AMD3100 in human with ischemic disease has not been reported. Given the high morbidity associated with ischemic diseases, it is very important to develop novel and effective small molecules that promote the mobilization of EPCs and angiogenesis in ischemic tissue.

Me6TREN (Tris[2-(dimethylamino)ethyl]amine, hereafter Me6) is a chemical compound that contains multiple hydrogen-bonding acceptor sites. It is frequently used as a ligand for the clean synthesis of functional polymers¹⁸. So far, the biologic activity of Me6 remains unclear. Recently, we have first reported the novel small



molecule Me6 had ability to effectively mobilize hematopoietic stem and progenitor cells (HSPCs)¹⁹. Interestingly, HSPCs share similar migration and adhesion properties with EPCs in the BM^{11,14,20,21}. Thus, we postulated that Me6 might induce EPC mobilization. In this study, we provided the first evidence that Me6 induced long-lasting and effective mobilization of EPCs from the BM into the blood circulation. Me6 itself showed therapeutic potential on ischemic tissue regeneration. Systemic administration of Me6 into mice with HLI significantly enhanced blood flow reperfusion, increased capillary density and regenerative muscle weight in the ischemic limbs through matrix metalloproteinase-9 (MMP-9) protease-dependent mechanism. Our results suggest that Me6 will be a potent and effective therapeutic molecule to promote ischemic tissue repair and regeneration.

Results

Me6 Induced a Long-Lasting EPC Mobilization. By using flow cytometry analysis, we found that mice injected with Me6 had increased number of Flk-1⁺, Sca-1⁺ and CD34⁺ cells in the PB (Fig. S1). Then we further explored the effective time and dose-response manner of Me6 on mobilizing Flk-1⁺Sca-1⁺ EPCs. We found a significant increase in circulating Flk-1⁺Sca-1⁺ cells at 12 h (3.59 ± 0.58 fold), 24 h (3.31 ± 0.82 fold) and 48 h (2.68 ± 0.48 fold) compared with 0 h post injection of Me6 (Fig. 1A). Until 72 h, EPCs in PB recovered to normal levels. Dose-response studies showed a clear dose-dependent effect with a peak increase of 4.25 ± 0.45 fold of Flk-1⁺Sca-1⁺ cells in PB at 12 h post subcutaneous injection of Me6 (10 mg/kg) compared with the control (Fig. 1B). In addition to observe the mobilization of EPCs into blood by Me6 (Fig. 1C), we evaluated the distribution of Flk-1⁺Sca-1⁺ cells in the spleen via flow cytometry. After injection of Me6 at 5 mg/kg, more Flk-1⁺Sca-1⁺ cells were detected in the spleen compared to the control group (Fig. 1D). We next used an endothelial colony assay to observe the mobilization effect of EPCs by Me6. Compared with the control group, much more EPC-CFU were detected in the PBMNC cultures derived from Me6-treated mice (Fig. 1E). These results suggest that Me6 may be a novel EPC mobilizing agent, which might have the function in promoting angiogenesis.

Me6-Mobilized EPCs Enhanced the Restoration of Blood Flow in Ischemic Hind Limbs. To test the function of Me6-mobilized EPCs in vivo, we prepared a HLI model by excising the left femoral artery from mice. 2 mL of Donor PB was collected at peak EPC mobilization time of Me6 at 12 h and AMD3100 at 1 h post injection. The flow cytometry results showed that Me6 mobilized slightly more numbers of Flk-1⁺Sca-1⁺ cells into PB than AMD3100 (Fig. 2A, B). MNCs were isolated from 2 mL mobilized PB and were then intramuscularly injected into the ischemic limbs. The LDPI results showed that the blood flow in ischemic limbs of mice transplanted with AMD3100- or Me6-mobilized MNCs recovered better than those of mice transplanted with the control group at 14 days post transplantation (Fig. 2C, D). The control group transplanted with PBMNCs from vehicle-treated mice, they presented a relatively slow and incomplete blood flow recovery in the ischemic limbs over 3 weeks. These results suggest that the circulating EPCs mobilized by Me6 have the ability to promote angiogenesis and improve blood flow recovery in ischemic tissue.

Systemic Administration of Me6 Promoted Angiogenesis. To further observe the therapeutic effect of Me6 on ischemic tissue repair, mice afflicted with HLI were subcutaneously injected with PBS, Me6 or AMD3100 at a concentration of 5 mg/kg once per week. First, flow cytometry analysis revealed the percentage of Flk-1⁺Sca-1⁺ cells in PB was significantly increased in all the groups at day 3 after HLI operation. Notably, Me6 induced much more number of EPCs into the blood circulation than AMD3100 at day

7 and day 14 after HLI operation (Day 7: Me6 6.75 ± 0.71% vs. AMD3100 2.90 ± 0.57%; Day 14: Me6 6.25 ± 0.81% vs. AMD3100 4.37 ± 0.71%) (Fig. 3A, B). We also observed the recovery of blood flow in ischemic limbs in response to each treatment (Fig. 3C). Both Me6 and AMD3100 significantly increased hind limb blood reperfusion relative to the controls from day 7 to 28 (Fig. 3C, D). Histological analysis of the ischemic hind limbs was performed 14 days after HLI with different treatment. Notably, the enhancement of capillary density as a result of Me6 treatment was significantly better than that of the control and the AMD3100-treated mice (Fig. 3E, F). The cell apoptosis rate of ischemic limb muscle was significantly decreased to 9.88 ± 1.50% in the Me6 group and 14.74 ± 2.21% in the AMD3100 group at 14 days (Fig. 4A, B). The capillary endothelial cells proliferation was further observed by using anti-BrdU and anti-BS-lectin 1 staining in ischemic muscle area. The number of BrdU⁺ BS-lectin 1⁺ cells was much higher in the Me6 group than the other groups (Me6 27.17 ± 7.22 vs. AMD3100 11.83 ± 2.04 vs. vehicle 3.00 ± 1.15) (Fig. 4C, D). In addition, Me6 injection induced significant recovery of blood reperfusion in ischemic limbs than AMD3100 treatment on day 21 and 28 after HLI (Fig. 3C, D). In addition, Masson's trichrome staining demonstrated that collagen fiber deposition in ischemic limb muscles was remarkably reduced in the Me6 group than the vehicle control and the AMD3100 groups (Fig. 4E, F). Me6 treatment conferred better long-term regeneration of muscle tissue, as assessed by the ratio of muscle weight in ischemic limbs to normal limbs at day 50 (Fig. 4G). These results suggested that Me6 persistently mobilized and recruited more EPCs into ischemic tissue than AMD3100, which significantly enhanced neoangiogenesis, reduced cell apoptosis and promoted muscle regeneration in mouse ischemic hind limbs.

Me6 Recruited Autologous BM-Derived EPCs to Ischemic Limbs.

To further demonstrate that the egress of EPCs from BM contributes to angiogenesis in ischemic limbs of mice following Me6 treatment, BM cells from GFP-transgenic mice were transplanted into lethally irradiated wild-type mice (Fig. 5A). Flow cytometry revealed that 85–90% of peripheral leukocytes from recipient mice were GFP⁺ (data not shown) after six weeks, suggesting that the BM of recipient mice was reconstituted by bone marrow transplantation (BMT). These mice were performed with HLI operation and different agent injection (Fig. 5A). The perfusion index of the Me6 treatment group was much higher than that of the AMD3100 group on day 14, 21 and 28 (Me6 0.88 ± 0.04 vs. AMD3100 0.75 ± 0.06 on day 28) (Fig. 5B,C). Me6 treatment significantly increased the capillary density of ischemic limbs and conferred better long-term regeneration of ischemic muscle tissue (Fig. 5D–F). BM-derived GFP⁺ cells were detected in ischemic area in each group, which were inserted partially into hybrid blood vessels among mouse vascular endothelium cells (Fig. 6A). Relative to the vehicle control and the AMD3100 group, Me6 treatment remarkably augmented the GFP⁺BS-lectin 1⁺ endothelial cells density (μm²/mm²) in ischemic tissues (Me6 13553.75 ± 1126.68 vs. AMD3100 8347.50 ± 1632.79 vs. vehicle 3858.75 ± 377.37) (Fig. 6B). Consistently, Me6 treatment showed the highest GFP⁺α-SMA⁺ arteriole density in ischemic regions (μm²/mm²) among all groups (Me6 115370.40 ± 1126.68 vs. AMD3100 81789.60 ± 3477.34 vs. vehicle 47254.80 ± 7618.24) (Fig. 6C, D). These results suggested that injection of Me6 was an effective way to recruit BM-derived progenitors into the ischemic tissues, increase capillary and arteriolar densities.

Me6 Reduced SDF-1α Level in the BM by Up-regulation of MMP-9 Expression.

To investigate the mechanism of EPC mobilization in response to Me6, we used ELISA to evaluate the dynamic change of stromal cell-derived factor-1α (SDF-1α) levels in the BM and PB after Me6 injection. From 12 h to 48 h post Me6 injection, we observed a significant reduction in the amount of SDF-1α protein

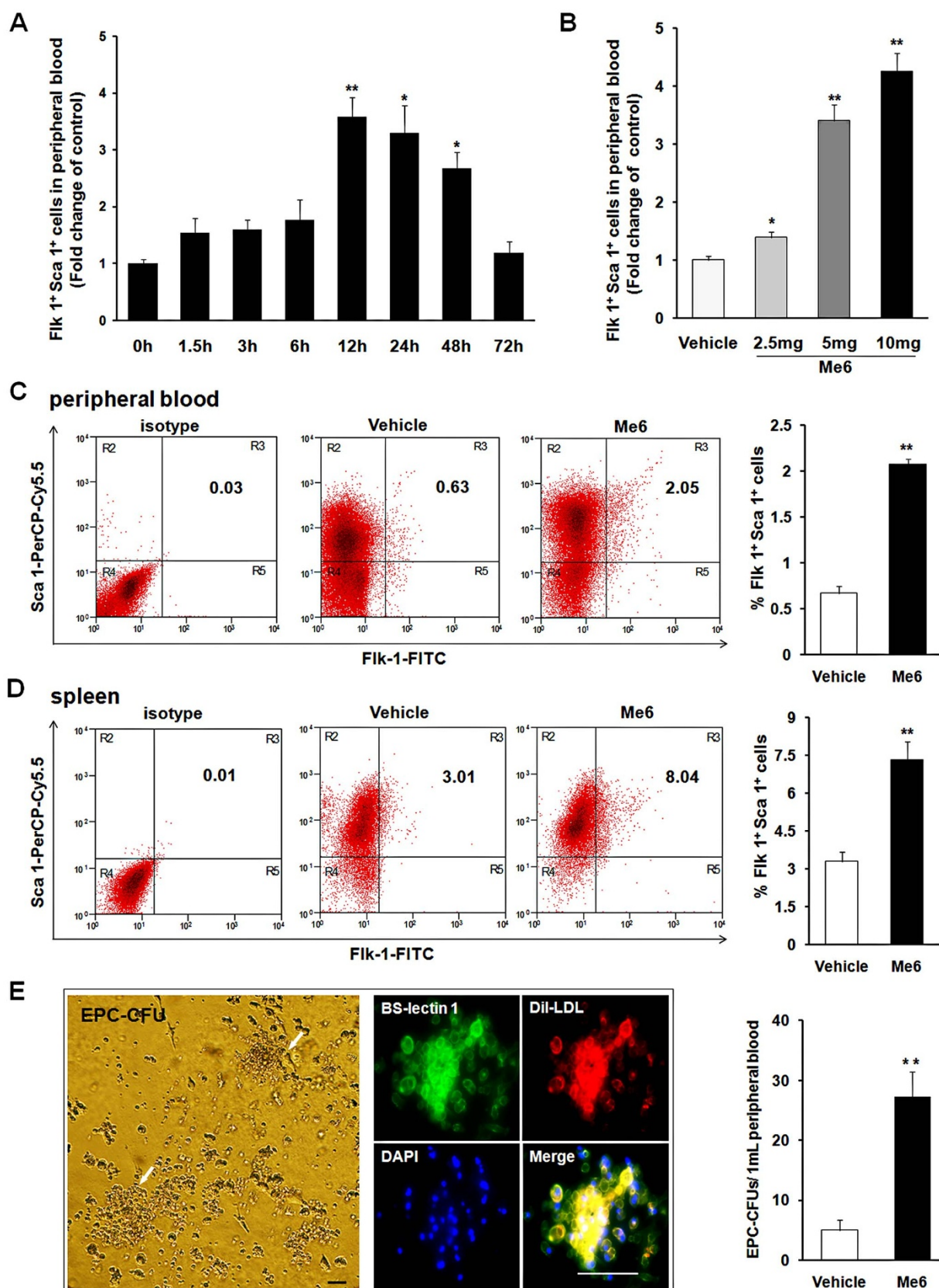


Figure 1 | Time and dose-response effects of Me6 on mobilization of EPCs into mouse PB. (A) Time-response effects of Me6 (5 mg/kg) on mobilization of EPCs into PB. (B) Dose-response effects of Me6 on mobilization of EPCs into PB. PB were collected at 12 h post injection of Me6 and analyzed for the percentage of Flk-1⁺ Sca-1⁺ cells by flow cytometry (n = 9 mice; *p < 0.05, **p < 0.01). (C–D) Representative FACS plots and mean percentages of Sca-1⁺ Flk-1⁺ cells on PBMCs and spleen cells were shown. Mouse PB and spleen cells were collected at 12 h post injection of Me6 at 5 mg/kg or PBS. (n = 9 mice; **p < 0.01). (E) EPC-CFUs emerged from cultures of Me6 or vehicle-mobilized PBMCs and identified by BS-lectin 1⁺ Dil-LDL⁺ cell colony units. The number of EPC colonies was counted after 12-day culture. (n = 6 mice; **p < 0.01; scale bar = 100 μm).

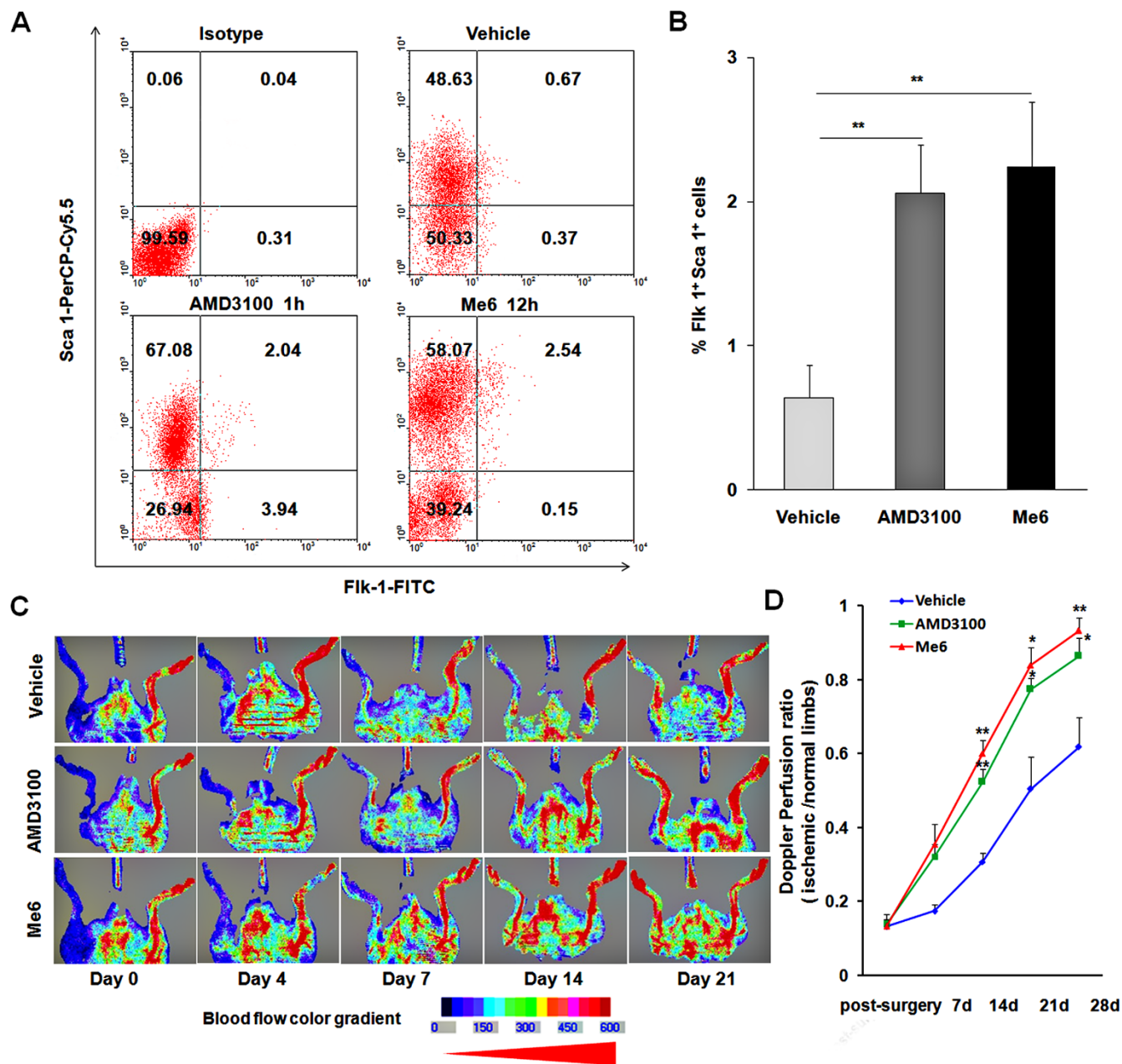


Figure 2 | Local transplantation of Me6-mobilized PB enhances blood flow restoration in hind limb ischemia model. (A, B) Flow cytometry analysis and quantitation of Flk-1⁺Sca-1⁺ cells on PBMCs 12 h post injection of Me6 or 1 h post injection of AMD3100 at 5 mg/kg (n = 9 mice; **p < 0.01). (C, D) LDPI showing recovery of blood flow after surgery and expressed as the ratio of perfusion in ischemic limbs to normal limbs (n = 6 mice; AMD3100 vs. vehicle control, Me6 vs. vehicle control, *p < 0.05, **p < 0.01). Mice with HLI were locally injected with 2 mL of PB-derived MNCs from vehicle control, Me6 or AMD3100 treated mice.

in the BM (Fig. 7A). Responsively, the expression of CXCR4 on BMMNCs from Me6 treated mice was significantly increased compared with the controls at 12 h post Me6 injection (Fig. 7B). A decrease in BM SDF-1 α levels has been reported to coincide with proteolytic activity of matrix metalloproteinase MMP-9^{21,22}. The ELISA results showed that the MMP-9 concentrations of BM supernatants increased from 6 h to 48 h following Me6 administration (Fig. 7C). Q-PCR analysis was performed to further evaluate the expression levels of MMP-9 mRNA in BM cells. The results showed that the levels of MMP-9 mRNA in mouse BM cells increased at 6 h, reached to a peak at 24 h post injection of Me6 and then gradually decreased to baseline levels (Fig. 7D). We also

performed in vitro experiments by culturing normal mouse BM cells and human umbilical vein endothelial cells (HUVECs) with Me6 treatment. Me6 significantly increased the expression level of MMP-9 mRNA in these cells (Fig. 7E, F). Importantly, Me6 treatment resulted in increased MMP-9 protein expression in HUVECs (Fig. S2), indicating the direct role of Me6 on MMP-9 expression.

In addition, flow cytometry analysis showed that Me6 failed to increase the percentage of circulating Flk-1⁺Sca-1⁺ cells in MMP-9 knockout mice (Fig. 7G). However, Me6 caused a significant mobilization of EPCs in wild-type mice (Fig. 7G). These results suggest that MMP-9 play a pivotal role in the process of Me6-induced EPC mobilization.

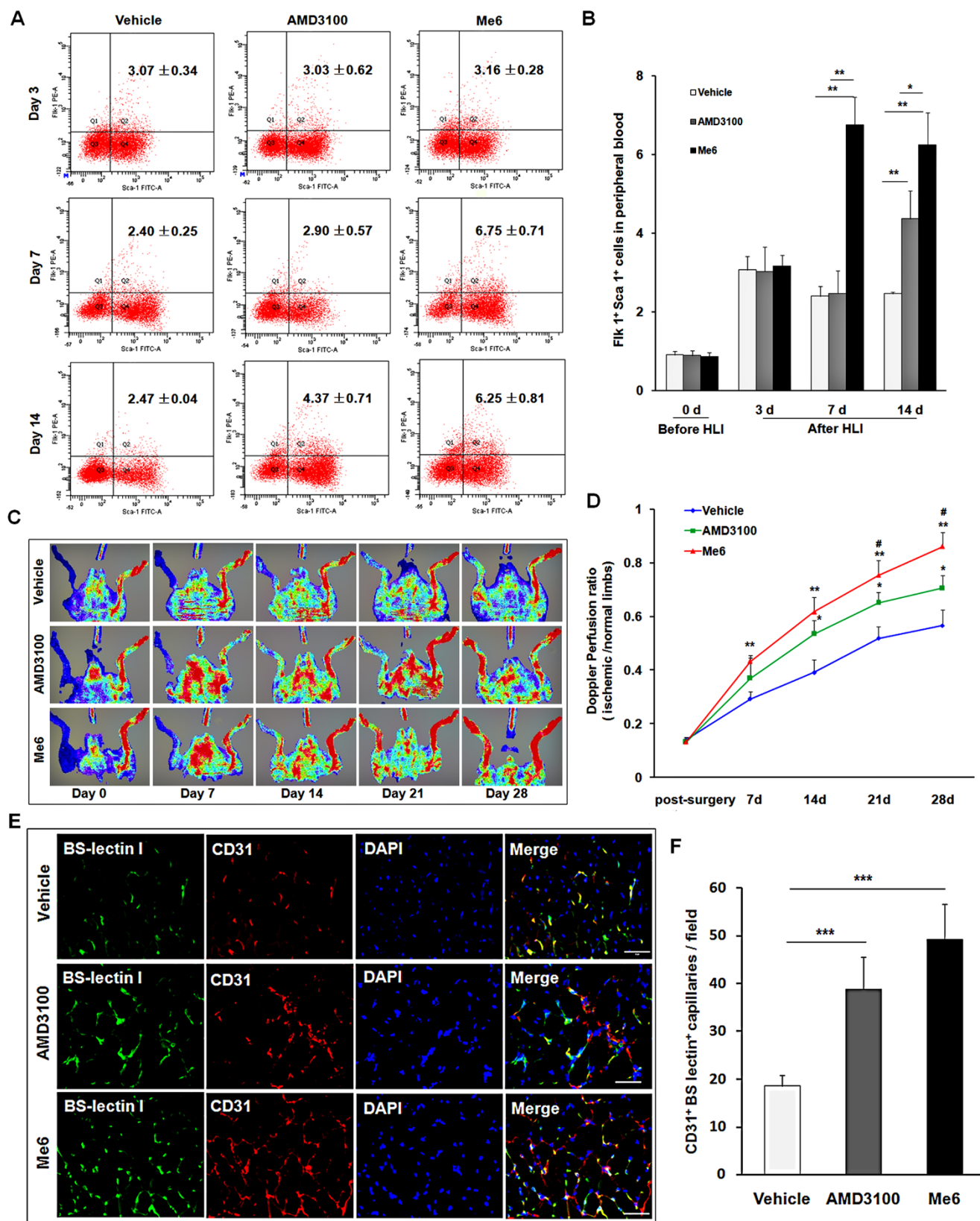


Figure 3 | Me6 stimulated the recovery of blood flow and increased capillary density after HLI. (A, B) Flow cytometry analysis and quantitation of Flk-1⁺Sca-1⁺ cells on PBMNCs at 3, 7, 14 days post injection of Me6 or AMD3100 in HLI mice (n = 5 mice; *p < 0.05; **p < 0.01). (C) Representative LDPI showed recovery of blood flow after HLI surgery and injection with different agent. (D) The ratio of the ischemic (left) to normal (right) limb blood flow was used for quantitative analysis (n = 15 mice; AMD3100 vs. vehicle control, *p < 0.05; Me6 vs. vehicle control, **p < 0.01; AMD3100 vs. Me6, #p < 0.05). (E) Representative fluorescent microscopy images of capillaries in gastrocnemius muscle sections (BS-lectin 1⁺, green; CD31⁺, red) at day 14 (scale bar = 50 μ m). Arrows indicate BS-lectin 1 and CD31 double-positive capillaries. (F) Overall the BS-lectin 1⁺CD31⁺ capillary density (n = 6 mice; *p < 0.05; ***p < 0.001) in the ischemic area.

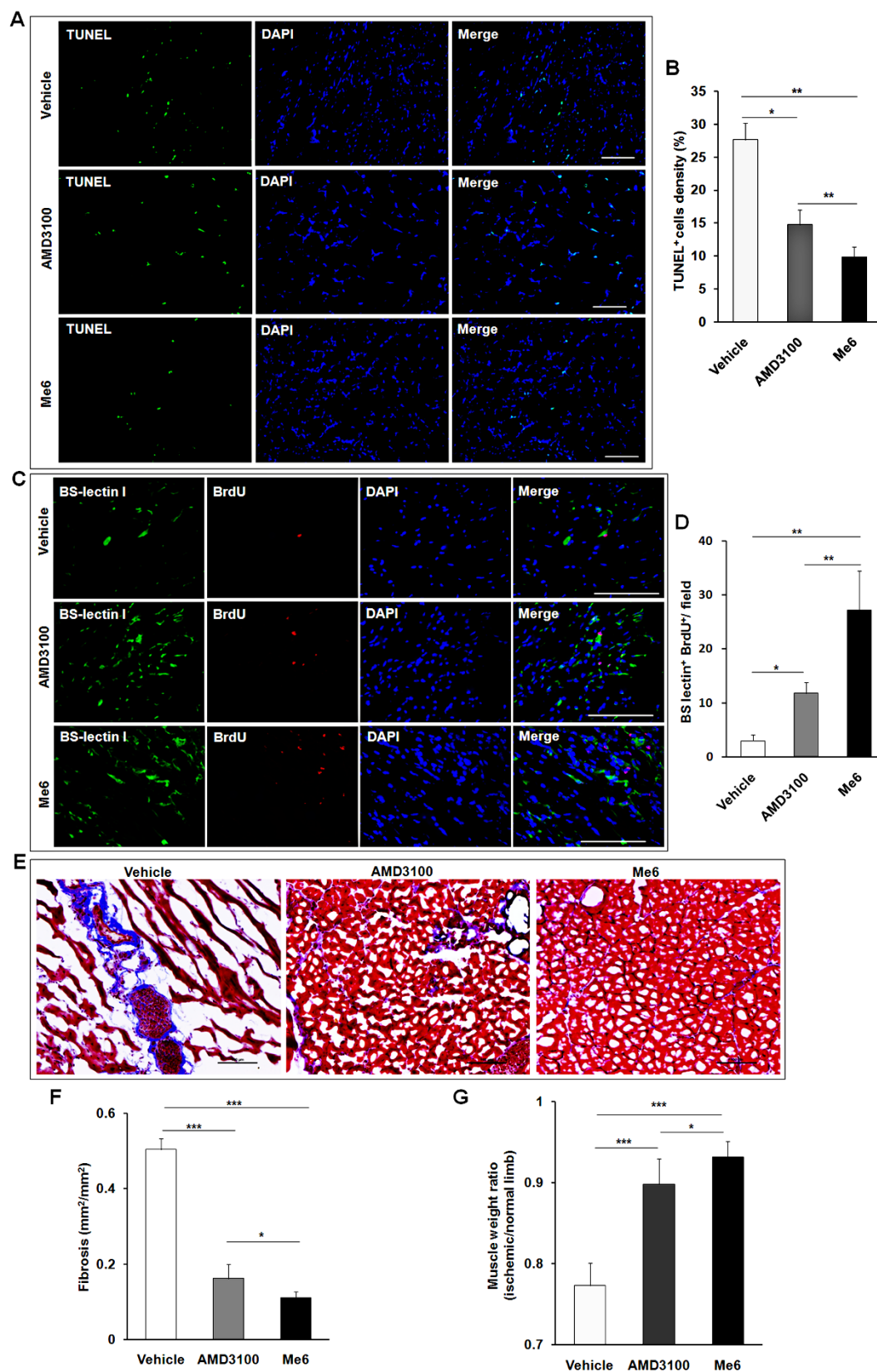


Figure 4 | Effect of Me6 on the angiogenic cell apoptosis and proliferation in ischemic limb. (A, B) Representative microphotographs of the section of ischemic muscles stained immunochemically for TUNEL. Quantitative analysis of TUNEL⁺ apoptosis cells in ischemic hindlimb muscles at day 14 (n = 6 mice; *p < 0.05, **p < 0.01; scale bar = 100 μ m). (C, D) Representative images of BrdU-DNA incorporation in BS-lectin 1⁺ endothelial cells in ischemic muscles at day 14. Quantitative analysis of BrdU⁺BS-lectin 1⁺ proliferative capillary endothelial cells (n = 6 mice in A–D; *p < 0.05, **p < 0.01; scale bar = 100 μ m). (E, F) Masson’s Trichrome staining (collagen stains as blue color) of ischemic muscle at day 14 (n = 6 mice; *p < 0.05, **p < 0.01; scale bar = 100 μ m). (G) Tissue preservation was expressed as the ratio of muscle weight in ischemic limbs to normal limbs. The mice were killed on day 50. The wet muscular tissue of the lower limbs was isolated and weighed (n = 6 mice; *p < 0.05, ***p < 0.001).

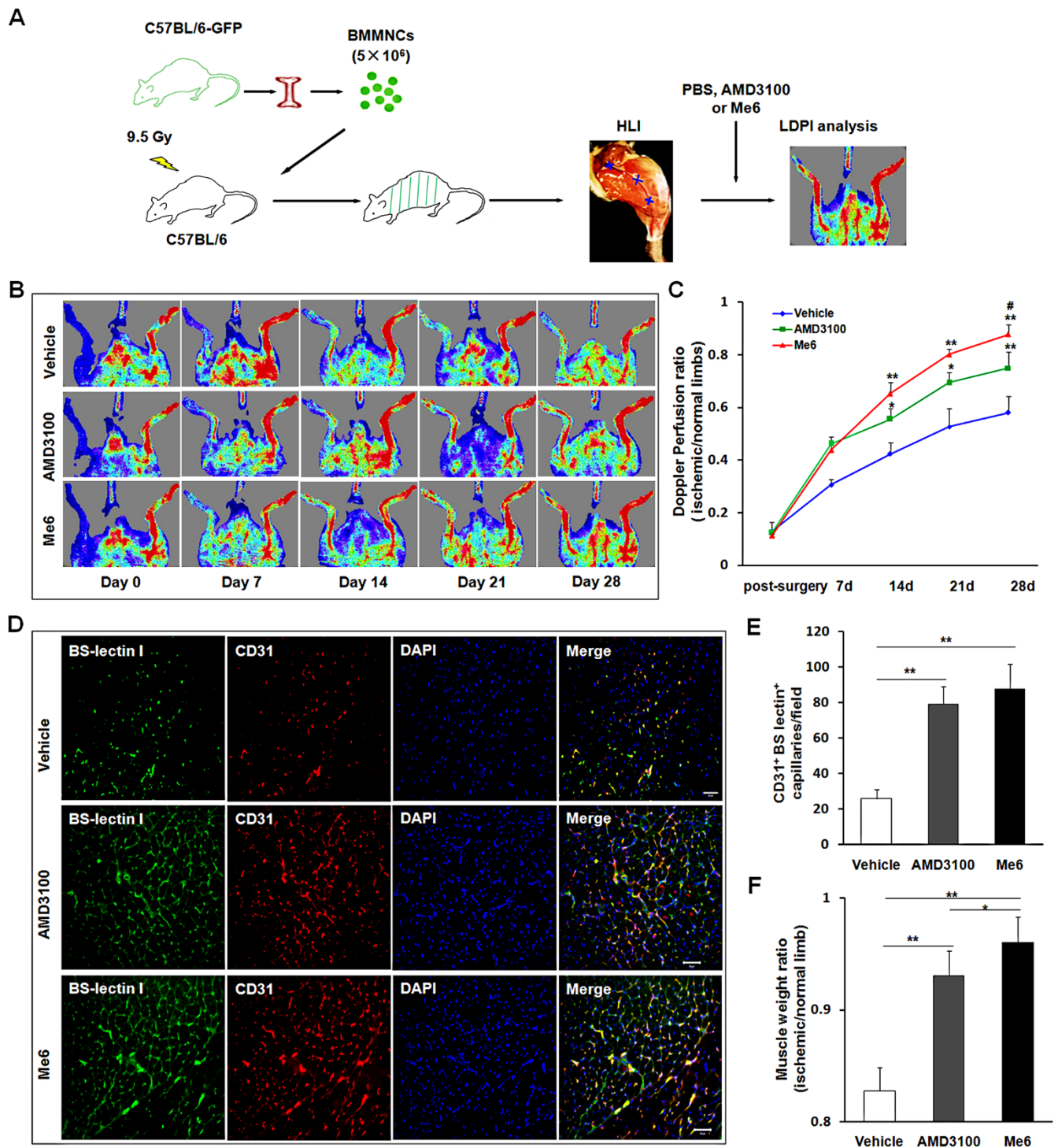


Figure 5 | Me6 enhanced the recruitment of BM-derived EPCs and angiogenesis in a HLI model. (A) Experimental protocol. 5×10^6 whole bone marrow cells from GFP-transgenic mice were transplanted into irradiated mice. Flow cytometry revealed that 85–90% of peripheral leukocytes from recipient mice were GFP⁺ at six weeks after BM reconstitution. Then these mice were performed with HLI operation and different agent injection one time per week. (B–C) Representative LDPI and mean blood flow perfusion ratio of mice with GFP⁺ BM cells replacement were analyzed after HLI surgery and injection with different agent ($n = 10$ mice; AMD3100 vs. vehicle control, $*p < 0.05$, $**p < 0.01$; Me6 vs. vehicle control, $**p < 0.01$; AMD3100 vs. Me6, $*p < 0.05$, $^{##}p < 0.01$). (D, E) Capillaries were identified by CD31 and BS-lectin 1 staining and quantitatively expressed as a capillary number per muscle fiber on day 28. Quantification of BS-lectin 1⁺CD31⁺ capillary density ($n = 6$ mice; $*p < 0.05$, $**p < 0.01$; scale bar = 100 μm). (F) The rest of the mice in each group were killed on day 50. A histogram expressed as the ratio of muscle weight in ischemic limbs to normal limbs ($n = 4$ mice; $*p < 0.05$, $**p < 0.01$).

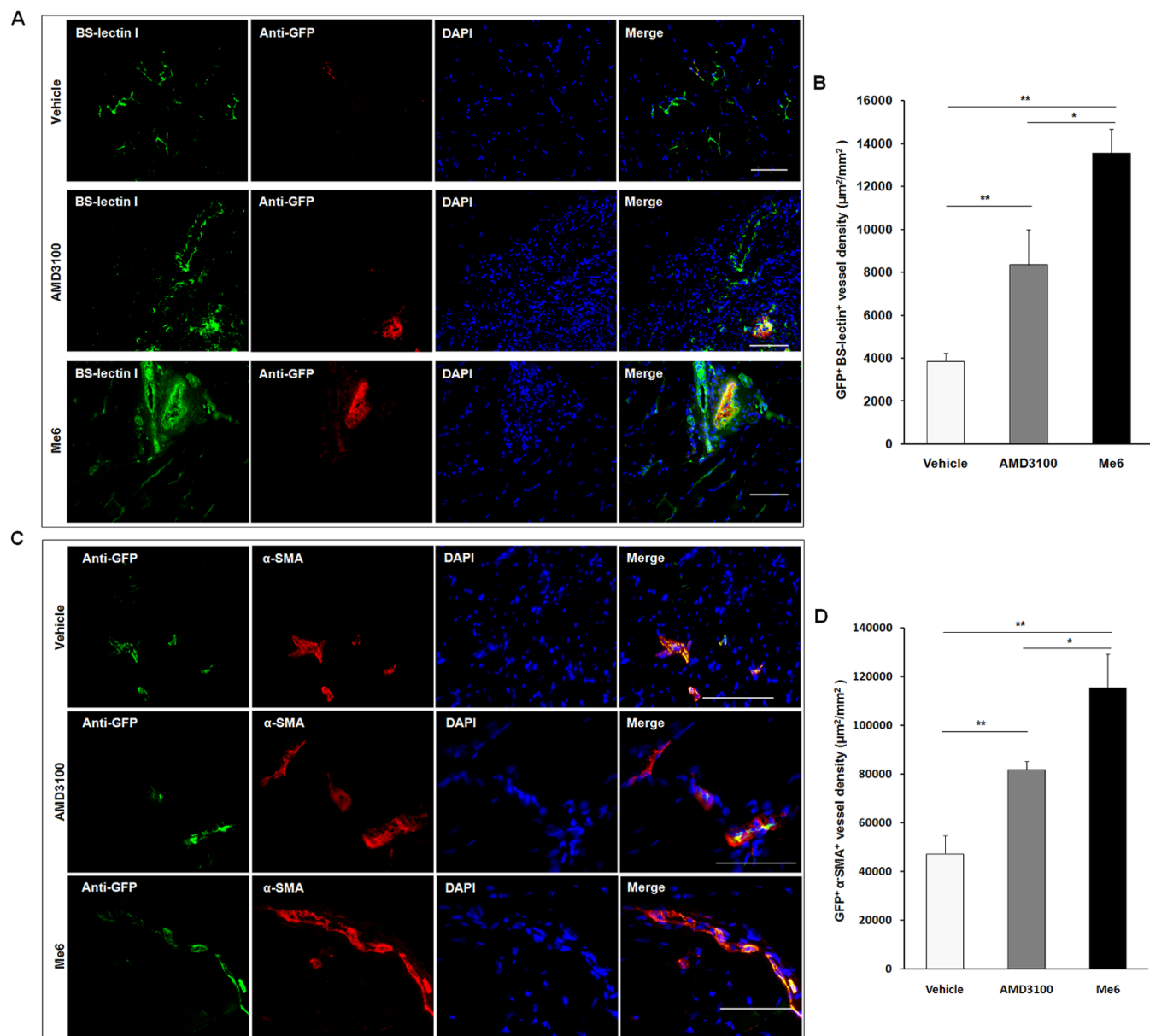


Figure 6 | Histological analysis of GFP⁺ cells in ischemic tissue after HLI. (A, B) Immunofluorescent double staining was used to analyze the GFP⁺BS-lectin⁺ cells in ischemic areas of the different groups and quantification of GFP⁺BS-lectin⁺ cells density (µm²/mm²) at day 28. (C, D) Immunofluorescent double staining was used to analyze the GFP⁺α-SMA⁺ cells in ischemic areas of the different groups and quantification of GFP⁺α-SMA⁺ vessel density (µm²/mm²) at day 28 (n = 5 mice in A–D; *p < 0.05, **p < 0.01; scale bar = 100 µm).

Discussion

Despite improvements in medical care and revascularization, patients with ischemic diseases continue to have a high risk of morbidity and mortality. Acceleration of angiogenesis is a critical point of treatment to enhance the outcome of ischemic diseases including stroke, myocardial infarction and peripheral arterial disease (PAD)^{1,23}. Of note, no medical therapies are effective in improving perfusion to the lower extremity in patients with PAD. Novel approaches for therapeutic angiogenesis can achieve the goal of restoring blood perfusion¹. Angiogenesis, the growth of new blood vessels from pre-existing vasculature in the body, which requires the migration, incorporation and differentiation of EPCs^{24,25}. This process plays a very important role in ischemic tissue regeneration. Several reports have suggested that angiogenesis of ischemic tissue was significantly improved by transplantation of BM or mobilized PB-derived EPCs^{23,26}. Compared with cell transplantation for ischemic tissue repair, systemic administration of drug with the abil-

ity to mobilize and recruit autologous EPCs to ischemic area is becoming a promising therapeutic strategy^{27,28}. Agents that can modulate the capillaries in ischaemic muscle in CLI could serve as goals for therapeutic angiogenesis. Therefore, there is substantial interest in the development of small molecules that can mobilize, recruit EPCs and enhance angiogenesis in ischemic tissue.

We first reported that Me6 has the capacity to effectively mobilize HSPCs into the blood circulation and showed no significant cytotoxic effect in the tested concentration range in vitro and in vivo¹⁹. We also found that Me6 showed the function on cellular protection, decreasing the apoptosis rate of serum-deprived HUVECs in a dose-dependent manner (Fig. S3). Compared with the median lethal dose (LD50) of AMD3100 at 16.3 mg/kg, Me6 exhibited a much lower toxicity with a LD50 value of approximate 1.11 g/kg in mice¹⁹.

In the present study, we found that a single injection of Me6 induced a significant increase in the percentage of circulating Flk-1⁺Scal⁺ cells, which reached peak mobilization at 12 h post-injec-

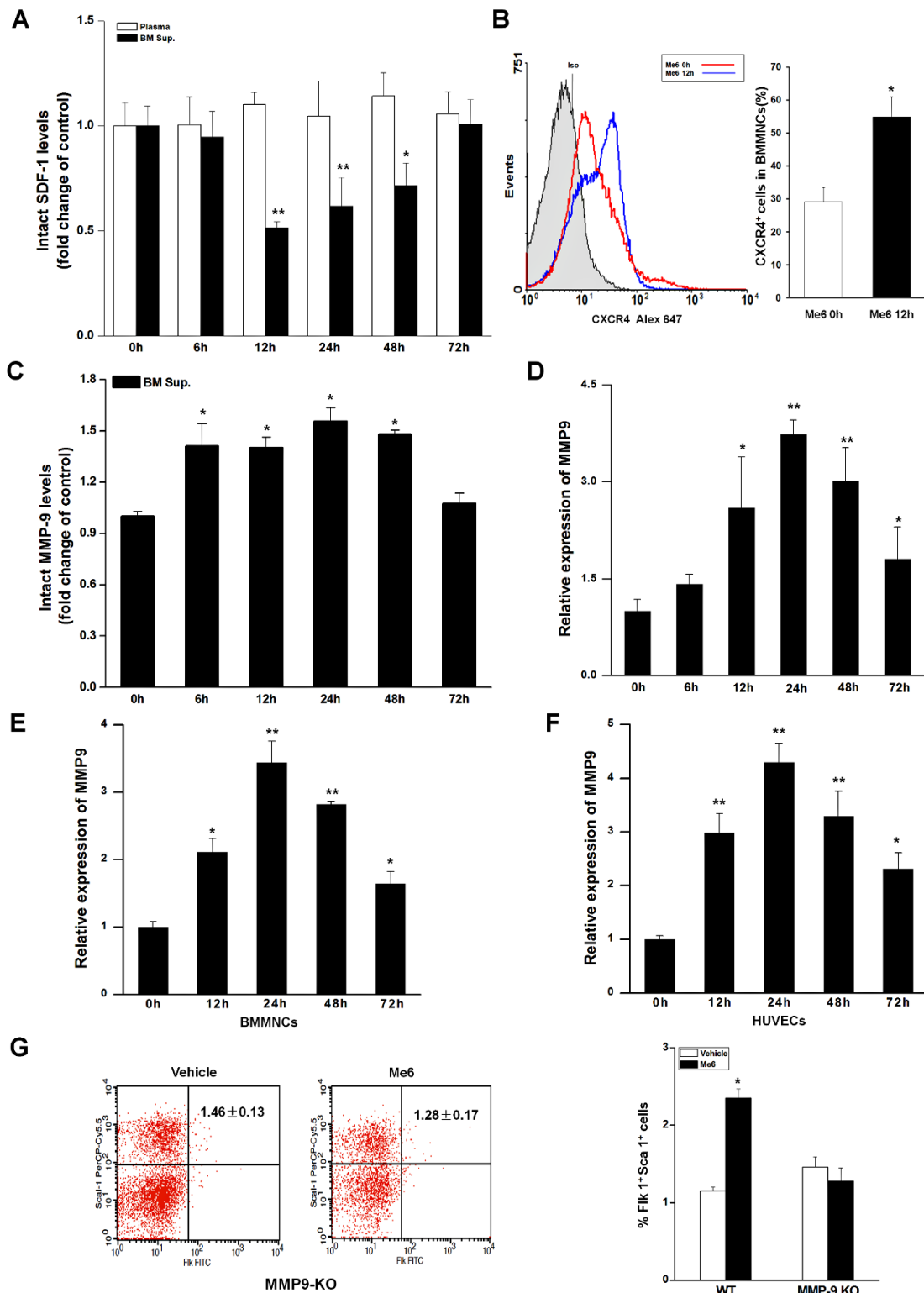


Figure 7 | Me6 reduced SDF-1 α level in the BM by up-regulation of MMP-9 expression. (A) Fold change in the levels of SDF-1 α protein in murine plasma and BM supernatants at 0–72 h post injection of Me6; the amount of SDF-1 α was detected by ELISA. (B) The percentage of CXCR4⁺ BMMNCs was measured by flow cytometry at 0 h or 12 h post Me6 injection. (C) Fold change in the levels of total MMP-9 in murine BM supernatants at 0–72 h upon administration of Me6; the amount of MMP-9 was detected by ELISA. (D) The expression of MMP-9 mRNA was up-regulated in BMMNCs derived from mice with Me6 injection. Mice were sacrificed at 0, 6, 12, 24, 48 and 72 h after Me6 injection and BMMNCs were isolated for Q-PCR analysis (n = 6 mice in A–D; *p < 0.05, **p < 0.01 vs. 0 h). (E, F) Me6 treatment up-regulated the expression of MMP-9 mRNA in mouse BMMNCs and HUVECs. Mouse BMMNCs and HUVECs were cultured with Me6 for 0, 12, 24, 48 and 72 h. RNA was extracted at different time point for Q-PCR analysis. (n = 6; *p < 0.05, **p < 0.01 vs. 0 h). (G) Me6 failed to increase the percentage of circulating Flk-1⁺Sca-1⁺ cells in MMP-9^{-/-} mice. MMP-9^{-/-} mice (KO) or wild-type (WT) mice were subcutaneously injected with 5 mg/kg Me6 or vehicle. PB were collected at 12 h post injection and were analyzed for the percentage of Sca-1⁺Flk-1⁺ cells by flow cytometry (n = 4 mice; *p < 0.05 vs. WT mice with vehicle treatment).



tion. The EPC mobilization caused by Me6 persisted for a long time, even more than 48 h. Repeated administration of Me6 (twice, 48 hours apart) also caused a significant EPC mobilization effect (Fig. S4), which suggested that the egress of EPCs into the blood was not desensitized by Me6 repeated treatment. The functional capacity of EPCs mobilized by Me6 was proved by their ability to enhance the restoration of blood flow in the murine HLI model. Importantly, we showed for the first time that systemic administration of Me6 markedly promoted angiogenesis and provided significant therapeutic benefit in ischemic limbs. Greater blood flow perfusion and higher capillary density were achieved via Me6 treatment than with AMD3100 especially at 14, 21 and 28 d post HLI operation, which might be due to the better mobilization effect on autologous EPCs caused by Me6. Notably, the increased presence of endothelial cells in the ischemic area of BM GFP⁺ cells-reconstructed mice after Me6 injection indicated that Me6 not only promoted the egress of BM EPCs into the circulation but that Me6 also facilitated the recruitment of them into the ischemic tissues. Therefore, Me6 showed the ability to enhance angiogenesis, reduce cell apoptosis and promote muscle regeneration in mouse ischemic hind limbs by utilization of an endogenous EPC repair mechanism. When HUVECs were plated on wells coated with Matrigel, the extent of tube formation was significantly increased in the presence of 100 μ M Me6 (vehicle 16.83 \pm 2.31 vs. Me6 33.33 \pm 3.88 branches/1000 μ m²) (Fig. S5). The data of Me6 in enhancing angiogenesis in vitro further supports a role for Me6 in promoting ischemic repair. In addition, we observed the presence of more CD29⁺CD105⁺ cells in the PB of Me6-treated group (Fig. S6), suggesting that Me6 mobilized and recruited more mesenchymal stem cells into the ischemic tissue than AMD3100. Our data further indicate that Me6 is a potent therapeutic candidate molecule for ischemic disease, through their recruitment of autologous stem or progenitor cells and enhancing angiogenesis without the need for exogenous cell transplantation.

Mechanistically, MMPs is involved in the degradation of the key substrates including vascular cell adhesion molecule-1, SDF-1 α to allow for migration of EPCs^{22,29–31}. The egress of EPCs from the BM to the PB is a crucial step for ischemic repair. The majority of this mobilization process is regulated by SDF-1 α , and its receptor CXCR4, which perform critical functions in the BM. Multiple studies suggested that the decreased SDF-1 α levels by MMP-9 in BM can mobilize EPCs^{32–34}. Our data collectively indicated that Me6 could directly up-regulate the expression levels of MMP-9 in BM cells. Cleavage of SDF-1 α by MMP-9 resulted in loss of binding to its cognate receptor CXCR4 on BM EPCs, which led to the dissemination of these cells from BM. Several reports suggested that the amount of SDF-1 α also affected the expression of CXCR4 on BM cells³³; and up-regulation of CXCR4 could be a consequence of the collapse of SDF-1 α concentrations in BM³⁵. Our data further supported the opinion that the increased CXCR4⁺ EPCs could be recruited to ischemic tissue and contribute to angiogenesis, where the SDF-1 α concentration was elevated. Our data suggest that Me6 is a potent and effective therapeutic molecule to promote therapeutic angiogenesis and achieve the goal of restoring perfusion for the ischemic diseases.

Conclusion

This study demonstrates that the novel small molecule, Me6, can induce long-lasting, effective mobilization and recruitment of autologous EPCs into ischemic tissues, enhance angiogenesis, reduce cell apoptosis and promote muscle regeneration in ischemic hind limb. The process is associated with increased levels of MMP-9 expression in BM cells and an interruption of the SDF-1 α /CXCR4 axis. It also provides a promising approach for therapeutic angiogenesis in other circumstances, such as stroke and myocardial infarction.

Methods

Animals. Adult C57BL/6 mice (8 weeks old, male, 20–25 g) were purchased from the China Academy of Medical Sciences Animal Center. GFP transgenic C57BL/6 mice were a kind gift from Professor Ming Fan (Institute of Basic Medical Sciences, Beijing, China). MMP-9^{-/-} mice (FVB strain) were purchased from ShangHai Biomedel Organism Science & Technology Development Company. Control FVB strain mice were purchased at 8 weeks of age from Beijing Vital River Laboratories.

All animal experiments were reviewed and approved by the animal center committee of Academy of Military Medical Sciences (Beijing, China) and followed the guideline of US National. Animals were housed and handled in accordance with the guidelines of the National Institutes of Health.

Mobilizing Agents. AMD3100 (Sigma) and Me6 (Sigma) were injected in the abdomen region subcutaneously. Because AMD3100 has been extensively used at this level, 5 mg/kg body weight was selected as the concentration to be used for both Me6 and AMD3100^{27,36,37}.

Flow Cytometry. Blood samples were collected in 0.1 M EDTA-2Na to prevent the blood clotting from the tail vein. After erythrocyte lysis, the viable lymphocyte population in peripheral whole blood was incubated with VEGFR-2-FITC (BD Pharmingen), Sca-1-PerCP-Cy5.5 (eBiosciences), and CXCR4-APC (eBiosciences) and then fixed in 1% paraformaldehyde. Flow cytometry analysis was performed with a FACS Calibur or FACS Canto II (BD Biosciences) using gates to exclude dead cells, debris, and platelets. Isotype control (eBioscience) antibodies were used to exclude false-positive cells.

EPC colony-forming Assay. To evaluate EPC colony forming units (EPC-CFUs) of PB, 1 \times 10⁶ PBMCs from vehicle control or Me6-injected mice were cultured in methylcellulose-containing medium M3236 (StemCell Technologies) with 20 ng/mL stem cell-derived factor, 50 ng/mL vascular endothelial growth factor, 20 ng/mL interleukin-3, 50 ng/mL basic fibroblast growth factor, 50 ng/mL epidermal growth factor, 50 ng/mL insulin-like growth factor-1 (all from R&D Systems), 2 U/mL heparin (Sigma-Aldrich), and 10% FBS (Gibco) for 10–12 days. After 10–12 days in culture, the EPC-CFU cultures were treated with 0.4 μ g/mL DiI-LDL (Biomedical Technologies) for 2 hour and fixed by application of 1 mL of 2% paraformaldehyde (PFA, Sigma-Aldrich) for 1 hour at room temperature. After a wash of the methylcellulose-containing medium with PBS, the cultures were reacted with FITC-BS-lectin 1 (Vector Laboratories) for 1 hour at room temperature. After a wash with PBS, the cultures were observed under a fluorescence microscope (IX70; Olympus). The number of EPC-CFUs reflected the number of primitive EPCs in the initial sorted cell fractions³⁸.

Bone marrow reconstitution. BMT was performed as previously described^{23,39,40}. The mice were sacrificed by cervical dislocation. Male C57BL/6 mice at 8 weeks of age were given a total dose of 9.5 Gy lethal radiation with a ⁶⁰Co source, as previously described⁴¹, and reconstituted via tail vein injection with 5 \times 10⁶ BM cells isolated from GFP-transgenic C57BL/6 donor femurs. Six weeks after the BMT, left hind limb ischemia was induced in the recipient mice. The reconstitution rate of the peripheral leukocytes was 85% to 90% as detected by flow cytometry⁴².

HUVEC culture. HUVECs were isolated from umbilical cords (kindly donated by Chinese PLA General Hospital) by enzymatic detachment using collagenase (SERVA Electrophoresis) as described elsewhere. Cells were routinely passaged in 0.2% gelatin-precoated (Sigma) polystyrene culture plates in EGM-2 Bulletkit (EBM-2 basal medium supplemented with the cytokine cocktail; LONZA) in a humidified atmosphere containing 5% CO₂. All experiments were conducted with HUVECs in passage 10.

The experiments using HUVECs were approved by the Ethics committee of the Academy of Military Medical Sciences (Beijing, China) and performed following the principles of the Declaration of Helsinki.

Murine hind limb ischemia model. HLI model was induced by ligation and excision of the femoral artery as previously described⁴³. In brief, eight-week-old male C57BL/6 mice were anesthetized via intraperitoneal injection with pentobarbital sodium (40 mg/kg body weight). An incision was made in the skin at the mid-portion of the left hind limb overlying the femoral artery. The femoral artery and vein were then dissected from the nerve and the proximal portion of the femoral artery and vein ligated with 6-0 silk sutures. The distal portion of the saphenous artery and vein and remaining arterial and venous side branches were ligated and then completely excised from the hind limb. For the first 2 days after the procedure, postoperative analgesia (buprenorphine 0.04 mg/kg body weight) was administered twice daily.

Laser Doppler Perfusion Imaging. To provide functional evidence for ischemia-induced changes in vascularization, laser Doppler perfusion imaging experiments were performed at 0, 3, 7, 14, 21 and 28 days as previously described^{25,44,45}, the ratio of ischemic to non-ischemic limb blood flow perfusions was measured with a laser Doppler perfusion image analyzer (LDPI; Moor Instruments).

Capillary Density. Immunofluorescence staining was performed as previously described⁴⁶. Capillary densities were compared in gastrocnemius muscle sections from control, Me6 or AMD3100-treated mice as previously described^{47,48}. BS-lectin 1 and anti-mouse CD31 antibody were used to identify endothelial cells in frozen tissue



sections. Capillaries were counted for each of 10 randomly chosen fields ($\times 200$) and the total number of capillaries was counted in each field.

Muscle fibrosis. To characterize the fibrosis of ischemic limb gastrocnemius muscles, tissues were prepared as described previously^{45,49}, and were stained with Masson's trichrome. Fibrotic tissues of all groups at 14 days after treatment were observed ($\times 100$). The area of fibrosis in 10 randomly chosen fields was analyzed as the mean per unit area (1 mm^2)⁵⁰.

TUNEL assay. Apoptosis of ischemic limb muscles was detected by DeadEnd™ Fluorometric TUNEL System (Promega) at day 14. The number of TUNEL⁺ nuclei and the total number of nuclei in the 10 different fields ($\times 200$) were counted by randomly chosen fields. TUNEL⁺ cell density (%) is expressed as the ratio of TUNEL⁺ nuclei to the total number of nuclei⁵¹.

BrdU cell proliferation assay. BrdU, a thymidine analog, is taken up by proliferating cells into cellular DNA. To monitor the proliferating capillary endothelial cells, the HLI mice were intraperitoneally injected with BrdU (100 mg/kg body weight) at day 13. The BrdU incorporation assay was performed using a cell proliferation assay kit (Sigma). The proliferating cells were counted for each of 10 randomly chosen fields ($\times 200$) in each field.

Tube formation assay. The formation of tube-like structures by HUVECs on an extracellular matrix (ECM)-like 3D gel consisting of Matrigel® (BD Biosciences) was performed as described⁵². The six-well multidishes were coated with growth factor-reduced Matrigel in according to the manufacturer's instructions. HUVECs (5×10^4) were incubated at 37°C for 24 h with Me6 treatment (0 or 100 μM) in 1 ml of DMEM. After incubation, HUVECs underwent differentiation into capillary-like tube structures. Tube formation was defined as a structure exhibiting a length four times its width. Tube formation was observed using an inverted phase-contrast microscope (Nikon). Representative fields were taken, and the average of the total number of complete tubes formed by cells was counted in 15 random fields by two independent investigators.

Enzyme-linked immunosorbent assay. Mouse SDF-1 α /CXCL12 and total MMP-9 concentrations were determined via an enzyme-linked immunosorbent assay (Quantikine; R&D Systems; MCX120). Samples of murine PB and BM were obtained at different time after Me6 injection. Serum was obtained from whole blood, whereas BM was processed as described previously³³. BM medullar samples obtained from centrifuged supernatants of BM cell suspensions (two femurs and tibias) were flushed in 500 μL PBS. Marrow cavity volumes were estimated to be 20 μL ^{53,54}, and the values were reported in molarity.

RNA isolation and quantitative PCR. BMMNCs and HUVECs were treated with Me6 (100 μM) for 0, 12, 24, 48 and 72 h in vitro. C57BL/6 mice were treated with Me6 (5 mg/kg body weight). The mice were then sacrificed by cervical dislocation and their BMMNCs were separated at 0, 6, 12, 24, 48 and 72 h. Total RNA was extracted with Trizol (Invitrogen) and Q-PCR analysis was performed as described previously¹⁹. The forward sequence of primer used for Q-PCR amplification of MMP-9 was 5'-TGACAGCGACAAGAAGTG-3', and the reverse sequence was 5'-CAGTGAAGCGGTACATAGG-3'. Glyceraldehyde 3-phosphate dehydrogenase (GAPDH) primers were used as control, the forward primer was 5'-GAGTCAACGGATTTGGTCTG-3', and the reverse primer was 5'-TTGATTTGGAGGGATCTCG-3'. All of the reactions were repeated at least three times.

Western Blot analysis. HUVECs were starved in serum-free DMEM for 4 h, stimulated with 0 μM or 100 μM Me6 for 24 h at 37°C. Cells were lysed in RIPA buffer (50 mM Tris-HCl, pH 7.5, 150 mM NaCl, 1% NP-40, 0.5% sodium deoxycholate, 0.1% SDS) and protease inhibitor cocktail Set I (Calbiochem). Clarified cell lysates were separated on SDS-PAGE (12% polyacrylamide) and transferred to polyvinylidene difluoride membranes (PVDF, BioRad). After soaking in blocking buffer, the membranes were incubated with anti-MMP-9 (Cell Signaling Technology) and anti- β -actin (Santa Cruz Biotechnology) antibodies overnight at 4°C. The membranes were washed with TBST and then incubated with horseradish peroxidase-conjugated secondary antibodies (Beijing Zhongshan Biotechnology) for 1 h at room temperature. After three additional washes with TBST, immunoreactive bands were detected using enhanced chemiluminescence (Santa Cruz Biotechnology), followed by exposure on BioMax film (Kodak).

Statistics. Data are presented as the mean \pm SD. Comparison between two means was performed with an unpaired Student's t test. Comparisons of more than two means were performed using ANOVA with Fisher PLSD and Bonferroni Dunn Post Hoc analysis. Statistical significance was assigned if $p < 0.05$.

- Annex, B. H. Therapeutic angiogenesis for critical limb ischaemia. *Nature Reviews Cardiology* **10**, 387–396 (2013).
- Qin, G. *et al.* Functional disruption of alpha4 integrin mobilizes bone marrow-derived endothelial progenitors and augments ischemic neovascularization. *J Exp Med* **203**, 153–163 (2006).
- Nolan, D. J. *et al.* Bone marrow-derived endothelial progenitor cells are a major determinant of nascent tumor neovascularization. *Genes Dev* **21**, 1546–1558 (2007).
- Yoder, M. C. *et al.* Redefining endothelial progenitor cells via clonal analysis and hematopoietic stem/progenitor cell principals. *Blood* **109**, 1801–1809 (2007).
- Foubert, P. *et al.* PSGL-1-mediated activation of EphB4 increases the proangiogenic potential of endothelial progenitor cells. *J Clin Invest* **117**, 1527–1537 (2007).
- Yamaguchi, J. *et al.* Stromal cell-derived factor-1 effects on ex vivo expanded endothelial progenitor cell recruitment for ischemic neovascularization. *Circulation* **107**, 1322–1328 (2003).
- Walter, D. H. *et al.* Sphingosine-1-phosphate stimulates the functional capacity of progenitor cells by activation of the CXCR4-dependent signaling pathway via the S1P3 receptor. *Arterioscler Thromb Vasc Biol* **27**, 275–282 (2007).
- Hu, J. *et al.* Analysis of origin and optimization of expansion and transduction of circulating peripheral blood endothelial progenitor cells in the rhesus macaque model. *Hum Gene Ther* **13**, 2041–2050 (2002).
- Fadini, G. P. *et al.* Peripheral blood CD34+KDR+ endothelial progenitor cells are determinants of subclinical atherosclerosis in a middle-aged general population. *Stroke* **37**, 2277–2282 (2006).
- Takahashi, T. *et al.* Ischemia- and cytokine-induced mobilization of bone marrow-derived endothelial progenitor cells for neovascularization. *Nat Med* **5**, 434–438 (1999).
- Pitchford, S. C., Furze, R. C., Jones, C. P., Wengner, A. M. & Rankin, S. M. Differential mobilization of subsets of progenitor cells from the bone marrow. *Cell Stem Cell* **4**, 62–72 (2009).
- Shepherd, R. M. *et al.* Angiogenic cells can be rapidly mobilized and efficiently harvested from the blood following treatment with AMD3100. *Blood* **108**, 3662–3667 (2006).
- Ozuyaman, B. *et al.* Nitric oxide differentially regulates proliferation and mobilization of endothelial progenitor cells but not of hematopoietic stem cells. *Thromb Haemost* **94**, 770–772 (2005).
- Moore, M. A. *et al.* Mobilization of endothelial and hematopoietic stem and progenitor cells by adenovector-mediated elevation of serum levels of SDF-1, VEGF, and angiopoietin-1. *Ann N Y Acad Sci* **938**, 36–45; discussion 45–37 (2001).
- Hristov, M., Zerneck, A., Liehn, E. A. & Weber, C. Regulation of endothelial progenitor cell homing after arterial injury. *Thromb Haemost* **98**, 274–277 (2007).
- Pitchford, S. C., Hahnel, M. J., Jones, C. P. & Rankin, S. M. Troubleshooting: Quantification of mobilization of progenitor cell subsets from bone marrow in vivo. *J Pharmacol Toxicol Methods* **61**, 113–121 (2010).
- Iwakura, A. *et al.* Estradiol enhances recovery after myocardial infarction by augmenting incorporation of bone marrow-derived endothelial progenitor cells into sites of ischemia-induced neovascularization via endothelial nitric oxide synthase-mediated activation of matrix metalloproteinase-9. *Circulation* **113**, 1605–1614 (2006).
- Eckenhoff, W. T. & Pintauer, T. Atom transfer radical addition (ATRA) catalyzed by copper complexes with tris[2-(dimethylamino)ethyl]amine (Me6TREN) ligand in the presence of free-radical diazo initiator AIBN. *Dalton Trans* **40**, 4909–4917 (2011).
- Zhang, J. *et al.* Small molecule Me6TREN mobilizes hematopoietic stem/progenitor cells by activating MMP-9 expression and disrupting SDF-1/CXCR4 axis. *Blood* **123**, 428–441 (2014).
- Salter, A. B. *et al.* Endothelial progenitor cell infusion induces hematopoietic stem cell reconstitution in vivo. *Blood* **113**, 2104–2107 (2009).
- Heissig, B. *et al.* Low-dose irradiation promotes tissue revascularization through VEGF release from mast cells and MMP-9-mediated progenitor cell mobilization. *J Exp Med* **202**, 739–750 (2005).
- Heissig, B. *et al.* Recruitment of stem and progenitor cells from the bone marrow niche requires MMP-9 mediated release of kit-ligand. *Cell* **109**, 625–637 (2002).
- Taguchi, A. *et al.* Administration of CD34(+) cells after stroke enhances neurogenesis via angiogenesis in a mouse model. *Journal of Clinical Investigation* **114**, 330–338 (2004).
- Carmeliet, P. Mechanisms of angiogenesis and arteriogenesis. *Nat Med* **6**, 389–395 (2000).
- Isner, J. M. & Asahara, T. Angiogenesis and vasculogenesis as therapeutic strategies for postnatal neovascularization. *J Clin Invest* **103**, 1231–1236 (1999).
- Higashi, Y. *et al.* Autologous bone-marrow mononuclear cell implantation improves endothelium-dependent vasodilation in patients with limb ischemia. *Circulation* **109**, 1215–1218 (2004).
- Capoccia, B. J., Shepherd, R. M. & Link, D. C. G-CSF and AMD3100 mobilize monocytes into the blood that stimulate angiogenesis in vivo through a paracrine mechanism. *Blood* **108**, 2438–2445 (2006).
- Zhou, B. *et al.* G-CSF-mobilized peripheral blood mononuclear cells from diabetic patients augment neovascularization in ischemic limbs but with impaired capability. *J Thromb Haemost* **4**, 993–1002 (2006).
- Nelson, A. R., Fingleton, B., Rothenberg, M. L. & Matrisian, L. M. Matrix metalloproteinases: biologic activity and clinical implications. *J Clin Oncol* **18**, 1135–1149 (2000).
- Levesque, J. P. *et al.* Mobilization by either cyclophosphamide or granulocyte colony-stimulating factor transforms the bone marrow into a highly proteolytic environment. *Exp Hematol* **30**, 440–449 (2002).



31. Pruijt, J. F. *et al.* Prevention of interleukin-8-induced mobilization of hematopoietic progenitor cells in rhesus monkeys by inhibitory antibodies against the metalloproteinase gelatinase B (MMP-9). *Proc Natl Acad Sci U S A* **96**, 10863–10868 (1999).
32. De Falco, E. *et al.* SDF-1 involvement in endothelial phenotype and ischemia-induced recruitment of bone marrow progenitor cells. *Blood* **104**, 3472–3482 (2004).
33. Petit, I. *et al.* G-CSF induces stem cell mobilization by decreasing bone marrow SDF-1 and up-regulating CXCR4. *Nat Immunol* **3**, 687–694 (2002).
34. Yokoi, H. *et al.* Bone marrow AT1 augments neointima formation by promoting mobilization of smooth muscle progenitors via platelet-derived SDF-1{alpha}. *Arterioscler Thromb Vasc Biol* **30**, 60–67 (2010).
35. Peled, A. *et al.* Dependence of human stem cell engraftment and repopulation of NOD/SCID mice on CXCR4. *Science* **283**, 845–848 (1999).
36. Broxmeyer, H. E. *et al.* Rapid mobilization of murine and human hematopoietic stem and progenitor cells with AMD3100, a CXCR4 antagonist. *J Exp Med* **201**, 1307–1318 (2005).
37. Liles, W. C. *et al.* Mobilization of hematopoietic progenitor cells in healthy volunteers by AMD3100, a CXCR4 antagonist. *Blood* **102**, 2728–2730 (2003).
38. Tsukada, S. *et al.* Identification of mouse colony-forming endothelial progenitor cells for postnatal neovascularization: a novel insight highlighted by new mouse colony-forming assay. *Stem Cell Res Ther* **4**, 20 (2013).
39. Fujita, J. *et al.* Administration of granulocyte colony-stimulating factor after myocardial infarction enhances the recruitment of hematopoietic stem cell-derived myofibroblasts and contributes to cardiac repair. *Stem Cells* **25**, 2750–2759 (2007).
40. Gong, Y., Fan, Y. & Hoover-Plow, J. Plasminogen regulates stromal cell-derived factor-1/CXCR4-mediated hematopoietic stem cell mobilization by activation of matrix metalloproteinase-9. *Arterioscler Thromb Vasc Biol* **31**, 2035–2043 (2011).
41. Du, N. *et al.* Radioprotective effect of FLT3 ligand expression regulated by Egr-1 regulated element on radiation injury of SCID mice. *Exp Hematol* **31**, 191–196 (2003).
42. Sahara, M. *et al.* Comparison of various bone marrow fractions in the ability to participate in vascular remodeling after mechanical injury. *Stem Cells* **23**, 874–878 (2005).
43. Couffignal, T. *et al.* Mouse model of angiogenesis. *Am J Pathol* **152**, 1667–1679 (1998).
44. Shao, H. *et al.* Statin and stromal cell-derived factor-1 additively promote angiogenesis by enhancement of progenitor cells incorporation into new vessels. *Stem Cells* **26**, 1376–1384 (2008).
45. Santulli, G. *et al.* CaMK4 Gene Deletion Induces Hypertension. *Journal of the American Heart Association* **1** (2012).
46. Zhou, J. *et al.* Fibroblastic potential of CD41+ cells in the mouse aorta-gonad-mesonephros region and yolk sac. *Stem Cells Dev* **21**, 2592–2605 (2012).
47. Oyama, O. *et al.* The lysophospholipid mediator sphingosine-1-phosphate promotes angiogenesis in vivo in ischaemic hindlimbs of mice. *Cardiovasc Res* **78**, 301–307 (2008).
48. Sumi, M. *et al.* Reconstituted high-density lipoprotein stimulates differentiation of endothelial progenitor cells and enhances ischemia-induced angiogenesis. *Arterioscler Thromb Vasc Biol* **27**, 813–818 (2007).
49. Yan, X. L. *et al.* Hepatocellular carcinoma-associated mesenchymal stem cells promote hepatocarcinoma progression: role of the S100A4-miR155-SOCS1-MMP9 axis. *Hepatology* **57**, 2274–2286 (2013).
50. Bhang, S. H. *et al.* Angiogenesis in ischemic tissue produced by spheroid grafting of human adipose-derived stromal cells. *Biomaterials* **32**, 2734–2747 (2011).
51. Kim, J. H., Jung, Y., Kim, B. S. & Kim, S. H. Stem cell recruitment and angiogenesis of neuropeptide substance P coupled with self-assembling peptide nanofiber in a mouse hind limb ischemia model. *Biomaterials* **34**, 1657–1668 (2013).
52. Santulli, G. *et al.* Evaluation of the anti-angiogenic properties of the new selective alphaVbeta3 integrin antagonist RGDechiHCit. *J Transl Med* **9**, 7 (2011).
53. Vogel, A. W. Comparison of simultaneously incurred damage to bone marrow and tumor tissue of animals treated with anticancer agents. *Cancer Res* **21**, 636–641 (1961).
54. Albanese, P. *et al.* Glycosaminoglycan mimetics-induced mobilization of hematopoietic progenitors and stem cells into mouse peripheral blood: structure/function insights. *Exp Hematol* **37**, 1072–1083 (2009).

Acknowledgments

We thank Dr. Jingyu Lin (Adverse Drug Reaction Monitoring Center, Beijing Drug Administration, China) for excellent technical assistance in Laser Doppler Perfusion Imaging. This work was supported by the National High Technology Research and Development Program of China (No: 2013AA020107; 2012AA020503) and National Basic Research Program of China (No: 2011CB964804; 2010CB945500).

Author contributions

H.X.C., Y.H.L. and X.T.P. conceived and designed the experiments; H.X.C., S.H.W., J.Z., X.L.R., R.Z., L.C., Y.L., L.J.H., Y.Z., W.S., B.W.Z. and X.N. performed the experiments; H.X.C., X.L.Y., W.Y., Y.H.L., X.T.P. analyzed the data; H.X.C. and Y.H.L. wrote the paper.

Additional information

Supplementary information accompanies this paper at <http://www.nature.com/scientificreports>

Competing financial interests: The authors declare no competing financial interests.

How to cite this article: Chen, H. *et al.* A novel molecule Me6TREN promotes angiogenesis via enhancing endothelial progenitor cell mobilization and recruitment. *Sci. Rep.* **4**, 6222; DOI:10.1038/srep06222 (2014).



This work is licensed under a Creative Commons Attribution-NonCommercial-NoDerivs 4.0 International License. The images or other third party material in this article are included in the article's Creative Commons license, unless indicated otherwise in the credit line; if the material is not included under the Creative Commons license, users will need to obtain permission from the license holder in order to reproduce the material. To view a copy of this license, visit <http://creativecommons.org/licenses/by-nc-nd/4.0/>